# EXPERIMENTAL INVESTIGATION OF MINIMUM ACHIEVABLE NOX FROM LOW CARBON FUELS

*Benjamin Emerson*[1,*], David Wu [2], David Noble [2], Robert Steele [2], and Tim Lieuwen[1]

[1]1Ben T. Zinn Combustion Laboratory, Georgia Institute of Technology, Atlanta, GA, USA
[2] EPRI, Charlotte, NC, USA

**Abstract.** Low carbon fuels face growing interest as the power generation and transportation fields embrace decarbonization. However, low carbon fuels may still introduce pollutant emissions challenges. Hydrogen and ammonia are two popular decarbonization fuels that face public scrutiny over potential $NO_X$ emissions. However, much of this scrutiny is grounded in unscientific roots, including experiments with improper control parameters or demonstrations with legacy hardware that are not appropriate comparison tests for these fuels. Therefore, EPRI and the Zinn Combustion Lab at Georgia Tech have conducted a series of chemical kinetic simulations and experiments with both hydrogen and ammonia to examine $NO_X$ emissions from direct combustion of these fuels with a target of dry, low $NO_X$ comparisons. The calculations were conducted to determine burner architectures that promise low $NO_X$ potential and fuel flexibility, as well as to predict the minimum achievable $NO_X$ ($NO_X$ entitlement). The experiments were conducted to validate the calculations and to provide first-ever demonstrations of a new fuel flexible, low $NO_X$ burner concept designed for these decarbonization fuels. This paper will present the promising calculations and experimental results. The results show hydrogen $NO_X$ emissions similar to natural gas combustion, and low double digit $NO_X$ concentrations from direct ammonia combustion.

## 1 INTRODUCTION

The existing fleet of gas turbine power generation assets plays an important role in the world's net zero future. This future role likely depends on gas turbine operation on renewable fuels with no or low carbon intensity. Hydrogen and ammonia are popular candidates as future land-based turbine fuels. However, these fuels have both faced scrutiny in public literature over concerns about potential $NO_X$ emissions with these fuels. However, these concerns are either speculative, rooted in data from early tests in legacy natural gas combustor hardware, or rooted in lab tests with inappropriate control parameters. In the case of hydrogen, $NO_X$ emissions concerns and misconceptions largely stem from non-premixed hydrogen-air considerations or fixed equivalence ratio considerations (rather than fixed firing temperature). In the case of ammonia, $NO_X$ emissions concerns stem from the potential for fuel-bound $NO_X$ produced by conventional combustor architectures.

Hydrogen is one promising decarbonization fuel. Gas turbines, which today constitute the dominant source of electric power in the US [1], have demonstrated immense reductions in the production of oxides of nitrogen ($NO_X$) emissions through the implementation of dry low-$NO_X$ (DLN) combustion technologies [2, 3, 4, 5, 6, 7, 8, 9]. The very premise for this $NO_X$ reduction is to control temperatures in the combustor, thereby controlling and limiting thermal $NO_X$ production. Recent efforts have demonstrated the feasibility of combusting hydrogen-doped natural gas in existing gas turbines [7, 10], presenting hydrogen as a viable solution for reducing carbon emissions within the existing energy infrastructure.

These efforts have not been without challenges. Hydrogen flames have the potential for higher temperatures and higher flame speeds as compared to methane flames. Part of this challenge relates to the connection of higher flame speeds and concerns about flashback in fuel-lean, premixed gas turbine combustors [11], prompting the gas turbine industry to develop methods to reduce this risk [5]. While doping fuels with $H_2$ has the capacity to reduce the amount of $CO_2$ and CO emitted by a ground-based gas turbine, many studies and non-scientific groups have postulated that due to having a higher flame temperature at a given equivalence ratio ($\varphi$), $H_2$-doped fuels will yield higher $NO_X$ emissions in the exhaust stream [4, 12, 13, 14, 15, 16]. However, this is not a relativistic comparison for how fuel replacement works for a gas turbine. Since these studies often do not compare the $NO_X$ emissions resulting from combustion of fuel blends of different hydrogen contents at the same flame temperature, the conclusions drawn obscure the actual influence of hydrogen addition on $NO_X$ formation. Several other studies have demonstrated that an increase in the hydrogen content in a hydrogen/natural gas fuel blend results in lower $NO_X$ emissions as compared to burning natural gas with the same flame temperature [6, 17, 18, 19]. These results emphasize the need for further experiments that compare measured $NO_X$ emissions for a range of hydrogen/natural gas fuel blends at fixed flame

* Corresponding author: bemerson@gatech.edu

temperatures representative of realistic turbine inlet conditions.

Many experimental studies in hydrogen research have investigated the effects of methane-hydrogen blending, but reporting emissions in terms of dry ppmvd corrected to 15% $O_2$. However, this is a biased comparison that artificially elevates the $NO_X$ reported for higher hydrogen fuels even for the same mass of $NO_X$ per unit of heat release. This is due to the different water content of the exhaust gas prior to drying, and it is also due to the different $O_2$ consumption of $H_2$ versus hydrocarbon fuels prior to the 15% $O_2$ correction. The result is a 40% bias towards higher $NO_X$ for $H_2$ fuels. This is detailed by Breer et al [20] and Douglas et al [21], who show that the relationship between concentration-based (ppmvd) and mass per unit energy-based (ng/J) $NO_X$ emissions reporting is not one-to-one. This demonstrates the potential for artificially inflated reporting of $NO_X$ emissions from $H_2$-blended fuels. Thus, there exists a need for unbiased reporting metrics for scientific $NO_X$ comparisons between fuel types. As detailed in Douglas et al [21], mass of $NO_X$ per unit energy can be calculated according to Eq 1. This equation takes the total mass flow rate of $NO_X$ calculated from the $NO_X$ concentration and the exhaust flow rate, and normalizes it by the rate of chemical heat input from the fuel. Douglas et al [21] also provide a way to convert between units of dry corrected ppmvd and mass of $NO_X$ per unit of energy, but this is more involved and is omitted here for brevity. In Eq 1, $\dot{m}_{NO_x}$ is the mass flow rate of $NO_X$, $\dot{Q}_{in}$ is the rate of chemical heat input of fuel, $\chi_{NO_X}$ is the $NO_X$ mole fraction, $\rho_{NO_X}$ is the $NO_X$ gas density, $\dot{V}_{exhaust}$ is the volume flow rate of exhaust, $\Delta h_c$ is the lower heating value of fuel, $\rho_{fuel}$ is the density of the fuel, and $\dot{V}_{fuel}$ is the volume flow rate of the fuel.

$$\frac{\dot{m}_{NO_X}}{\dot{Q}_{in}} = \frac{\chi_{NO_X}\rho_{NO_X}\dot{V}_{exhaust}}{\Delta h_c \rho_{fuel}\dot{V}_{fuel}} \qquad \text{Eq 1}$$

Previous work in hydrogen combustion research has used chemical kinetic calculations to compare $NO_X$ emissions of premixed hydrogen-air combustion to that of premixed methane-air combustion. Breer et al [20] performed this comparison with a chemical kinetic simulation with relevant control parameters, namely fixed residence time and flame temperature. Their work showed comparable NO emissions for premixed hydrogen-air flames compared to premixed methane-air flames. In the case of high power conditions (elevated combustor inlet temperature and pressure) hydrogen produced slightly lower NO than methane at the same flame temperature and residence time. This is due to the dominance of the thermal $NO_X$ mechanism for relevant residence times, and its relative insensitivity to fuel composition. This point is the very hypothesis that motivated this study.

Like hydrogen, numerous experimental studies have investigated ammonia combustion, particularly premixed combustors at atmospheric pressure and a range of equivalence ratios [22, 23, 24, 25]. This foundational work uncovered two important themes. First, the fuel-bound nitrogen in ammonia precludes lean premixing as a low $NO_X$ strategy due to the in-flame $NO_X$ production that dwarfs the thermal $NO_X$ production. The second important observation was the low $NO_X$ produced under rich conditions where equilibrium $NO_X$ concentrations are low. However, under rich conditions ammonia slip, combustion efficiency, and $N_2O$ emissions present other pollutant emissions concerns. These observations underline the need for a new combustor architecture for low $NO_X$ with ammonia.

The challenge of $NO_X$ emissions with ammonia combustion in legacy combustor architectures motivates a new architecture for ammonia combustion. In the 2023 ETN meeting, Gubbi et al. [26] presented a concept with a rich primary zone, a long residence time relaxation zone, and a lean burnout zone (secondary zone). A chemical kinetic simulation coupled with a NO minimization optimization revealed an optimal combustor configuration that minimizes NO with long residence times, high temperatures, and high pressures. Pressure is a particularly sensitive parameter because it provides lower rich equilibrium NO concentrations, and it accelerates the rate of relaxation to equilibrium. Figure 1 shows the pressure effect on predicted NO concentration. This configuration is notably in opposition to NO minimization trends with familiar lean premixed strategies. The study showed theoretical $NO_X$ entitlement as low as sub-30 ppm. An important contribution of this paper is to present an update to these calculations with recent experimental data.

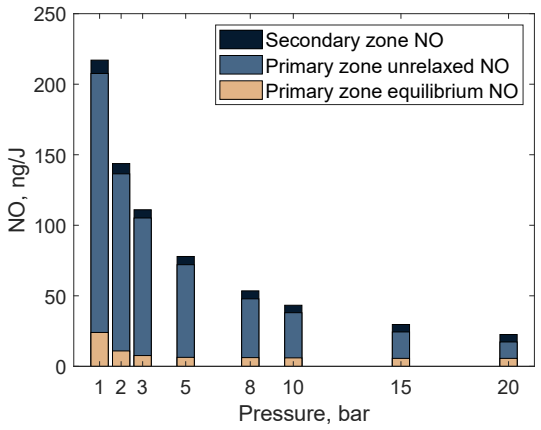


**Figure 1.** $NO_X$ production budget for an ammonia combustor with a rich primary stage and a lean secondary stage at a combustor exit temperature of 1900 K, re-plotted from the data from Gubbi et al **[26]**.

A commonly discussed concern with no-carbon fuels is their potential $NO_X$ emissions. However, recent chemical kinetic calculation studies have shown that $NO_X$ emissions should be manageable with these fuels. In the case of hydrogen, these studies show that lean premixed hydrogen combustion is expected to provide similar, and possibly lower, $NO_X$ emissions as lean premixed methane combustion at the same flame temperature and residence time. In the case of ammonia, these studies show that new combustor architectures may provide a low $NO_X$ solution despite the fuel-bound

nitrogen. This paper details experimental measurements that aim to demonstrate these calculated trends. The rest of the paper is organized with a summary of hydrogen combustion tests first, and then ammonia combustion tests second. Both of these experimental endeavours make progress on the characterization of $NO_X$ emissions of these fuels; the experiments make important insights but also identify additional future work to be done.

## 2 Hydrogen Combustion Testing

A hydrogen combustion test rig and emissions sampling apparatus were designed to experimentally investigate hydrogen combustion $NO_X$ in comparison to methane combustion $NO_X$. The design philosophy of this system was that it must be able to run lean, well-premixed fuels. It must be fuel flexible, and it must be able to sample $NO_X$ at different residence times to a) provide comparable residence times between different fuels, and b) to provide an indication of the thermal $NO_X$ production rate.

### 2.1 Experimental Setup

The test rig consisted of a sintered plate burner with the objective to provide a flat flame. A flat flame provides a uniform residence time, and it avoids localized stoichiometry inhomogeneity due to thermodiffusive effects. Therefore, fuel and air were premixed upstream of a stainless steel sintered plate, and a flame was stabilized downstream of the sintered plate. In order to ensure mixing, the air-fuel mixture was passively mixed along a mixing section of 86 hydraulic diameters with a Reynolds number of approximately 20,000 and steel-wool packing to agitate the mixture and reduce flammable volume. A quartz tube combustor liner was attached to the sintered plate burner to confine the combustion volume while providing optical access. Figure 2a shows a photograph of the sintered plate burner, and Figure 2b shows a photograph of a methane flame stabilized in this burner. The methane flame was selected to show here due to its optical emission in the visible spectrum and ease of imaging. The methane flame was additionally selected to demonstrate the presence of thermodiffussive instabilities, which are evident in the peak and valley structure of the nominally flat flame. This is important because thermodiffusive instabilities introduce non-uniformity of equivalence ratio. As hydrogen fraction is increased, the flame becomes more thermodiffusively unstable and this effect is amplified; therefore, the methane case provides an indication of the “best case” uniformity.

The sintered plate burner and quartz tube liner were installed in an optically accessible pressure vessel for testing at elevated pressure. A water-cooled traversable emissions probe was installed through the pressure vessel exhaust flange. This probe was traversed to different axial positions (in order to vary sampling residence time) by a hydraulic actuator system. The water cooled tip was designed to freeze the $NO_X$ chemistry at the point of sampling, and its temperature was monitored by a K-type thermocouple to ensure the probe temperature was sufficiently low to freeze NO formation, but sufficiently high as to maintain water in the gas phase.

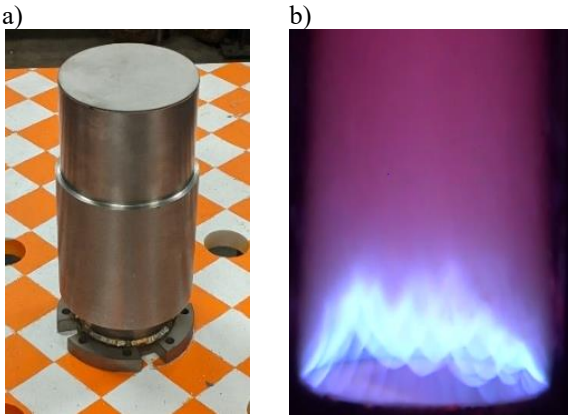


**Figure 2.** Photographs of the burner, showing a) sintered plate burner outside of the pressure vessel, and b) methane flame shape

The fuel and air supply to the rig consisted of high pressure lines of natural gas, hydrogen, and air. High pressure air is metered with a vortex flow meter. Natural gas and methane are metered independently with calibrated critical orifices and then blended. Water lines are also plumbed to the rig for the sampling probe, which is detailed next. Figure 3 shows a detailed plumbing and instrumentation diagram, detailing the air/fuel supply as well as the emissions sampling probe and its water cooling system.

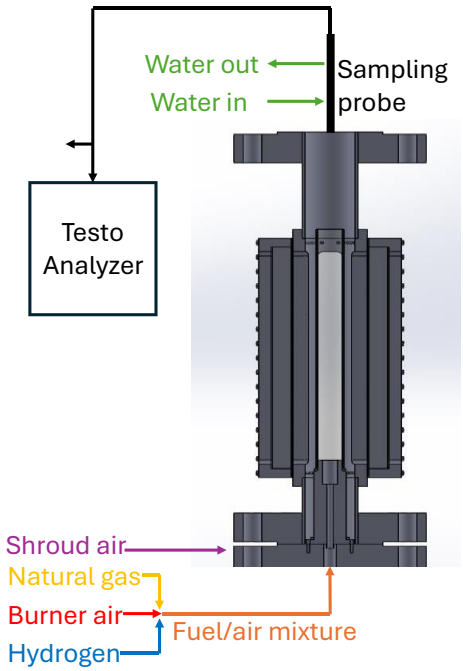


**Figure 3.** Plumbing diagram of hydrogen combustion test rig.

The combustor can be operated at a range of fuel gas blends from 100% methane to 100% hydrogen, and at variable equivalence ratios. The adiabatic flame

temperature is an important control parameter in these experiments, so the fuel gas mixture was balanced against the equivalence ratio to control a fixed flame temperature. Combustor pressure was also a variable in these experiments. In order to maintain combustor operability, it was important to be able to control combustor pressure independently of the flow rate through the sintered plate injector. Therefore, a shroud air line was incorporated to help control combustor pressure. This air mixes with the burned gases downstream of the quartz tube and upstream of the pressure vessel choke; therefore, the shroud air flow rate is a convenient parameter to control the chamber pressure independently of the flow through the fuel sintered plate and quartz tube liner.

The product gas was sampled by a water-cooled stainless steel probe, which could sample emissions at different residence times by moving the probe with an actuator. A triple concentric design uses water to cool the probe tip to quench the $NO_X$ chemistry at the point of sampling. Experiments were conducted with stainless probes, and later with quartz-tipped probes to further limit $NO_X$ chemistry in the probe. The results presented here were measured with the stainless probe; the quartz-tipped probe is a more recent but noteworthy development.

The sampled product gas was dried by a coil condenser, and a Testo 350 Flue Gas Analyzer measured the emissions. The Testo 350 has an instrumentation error of 0.2% for $O_2$ and 5 ppm for $NO_X$. The $NO_X$ reported is total $NO_X$ (NO and $NO_2$). Before each day of experimentation, the emissions analyzer was calibrated with span gas. All calibration gases had an error of +/- 2%. Lastly, a "zero" span gas test was also conducted, using ultra-pure nitrogen. Tests were also performed to analyze the effects of shroud air flow rate and probe coolant flow rate on $NO_X$ emissions. These tests showed that $NO_X$ emissions were insensitive to both shroud air flow rate and coolant flow rate within experimental uncertainty. Despite NO being the dominant oxide of nitrogen in the post-flame regions of gas turbine-like combustors, quenching the sample to a lower temperature means that this study must consider both the concentration of NO and $NO_2$. However, the total $NO_X$ produced is unchanged by the quench process, as the quench process excites reactions that convert NO to $NO_2$. As a result, this study must consider both NO and $NO_2$ to understand NO formation in the post-flame region. It is noteworthy that some $NO_2$ may be lost in the condensate from the exhaust sample; the reported data does not include an attempt to correct for this.

## 2.2 Results and Analysis

The hydrogen combustion tests were conducted by holding a fixed pressure and a fixed fuel gas composition. For each fuel gas composition, the adiabatic flame temperature was held constant by adjusting the equivalence ratio. For each fuel gas composition, the pressure was held constant by adjusting the shroud air flow rate. Next, for each fuel composition, a residence time sweep was conducted by traversing the axial position of the emissions probe. Probe position was converted to residence time based on a bulk velocity calculated from the mass flow rate, adiabatic burned gas density, and quartz tube cross-sectional area.

Several operability challenges were identified at extreme operating conditions. First, 100% hydrogen proved challenging at conditions matching lower hydrogen fractions due to flashback. During 100% hydrogen cases, the flame sits close to the sintered plate. Although the sintered plate is an effective flashback arrester, it gradually heats up during long test durations and eventually ignites the combustible mixture on the upstream side. Uncertainty management was the greatest challenge in these tests. This is due to the high exponential sensitivity of the thermal $NO_X$ production rate to the adiabatic flame temperature (and consequently to the equivalence ratio). This sensitivity is such that just a 5% uncertainty in fuel flow rate translates to a 100% uncertainty in thermal $NO_X$ production rate at a relevant range of flame temperatures (see Figure 4). This was a challenge because the extreme corners of the pressure-equivalence ratio-fuel gas composition have very different requirements for the individual fuel gas constituents. In other words, a high pressure, high equivalence ratio, high hydrogen case has extremely different fuel orifice requirements than a low pressure, low equivalence ratio, high methane case. The project included attempts to swap out various orifice combinations at different operating conditions, but this was extremely limiting with the available orifices and instrumentation. Therefore, in order to reasonably bound uncertainty in the adiabatic flame temperature (with regard to the thermal $NO_X$ production rate), results are only presented here for 30% and 50% hydrogen-to-methane blend ratios by volume. This was a disappointing limitation in this experiment and it may be responsible for the limited hydrogen effects that we observed. Future experiments are planned with Coriolis meters for improved measurement uncertainty to expand these ranges, although even with Coriolis meters the dynamic range of fuel flow rates remains a challenge.

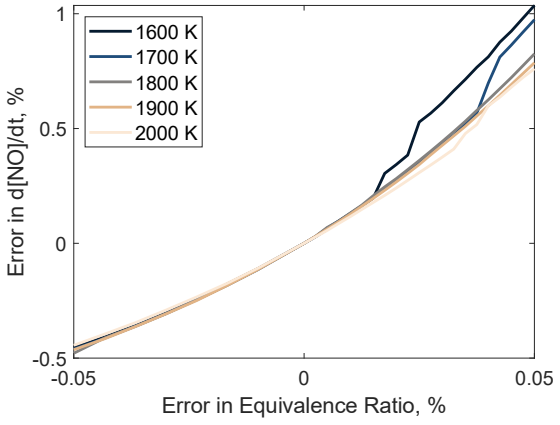


**Figure 4.** Calculated sensitivity of NOx production rate error to equivalence ratio error for methane-air combustion

Breer et al [20] and Douglas et al [21] showed that the relationship between concentration-based (ppmvd) and mass per unit energy-based (ng/J) $NO_X$ emissions

reporting is not one-to-one, demonstrating the potential for artificially inflated reporting of $NO_X$ emissions from $H_2$-blended fuels. This bias is particularly sensitive to hydrogen content, so hydrogen $NO_X$ results are presented in this paper on a mass per unit energy basis. $NO_X$ results at a combustor pressure of 5 bar and an adiabatic flame temperature of 1750 K are presented in Figure 5. The first and most important observation is the low single digit $NO_X$ emissions even in the case of 50% hydrogen; this re-emphasizes the point that $NO_X$ emissions is not an inherent issue with hydrogen combustion for an appropriately engineered burner.

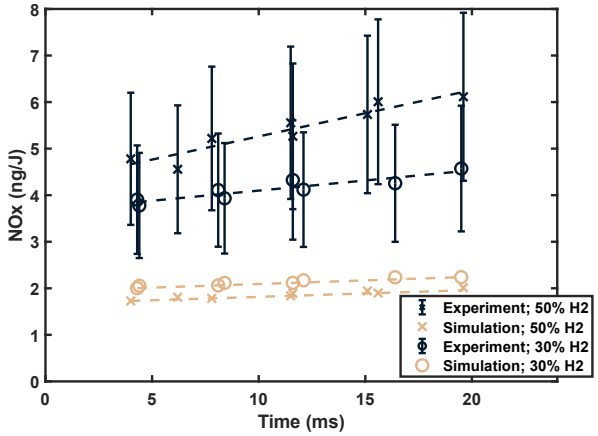


**Figure 5.** $NO_X$ vs residence time for methane-hydrogen blends consisting of 30% hydrogen and 50% hydrogen, and comparing experimental measurements to kinetic calculations. Combustor pressure is 5 bar and adiabatic flame temperature is fixed at 1750 K. Calculated values included from Breer et al **[20]**.

Another observation from the data in Figure 5 is that the measured $NO_X$ emissions are higher in the experiments than in the calculations. Coupled with this observation is the $NO_X$ production rate which is indicated by the slope of the $NO_X$ concentration dependence on residence time. Despite the careful control of the adiabatic flame temperature, it is evident that the thermal $NO_X$ production rate is higher in the experiments, and it is higher in the 50% hydrogen case than the 30% hydrogen case. This indicates a higher effective adiabatic flame temperature in the experiments, and more so in the higher hydrogen case. This could be attributed to experimental uncertainty due to the extreme sensitivity of thermal $NO_X$ production rate to measured fuel flow rate. However, the hypothesis is that corrugation of the flame by thermodiffusive instabilities produces inhomogeneity of temperature and consequently thermal $NO_X$ production rate, which is more severe in the higher hydrogen case which is more thermodiffusively unstable. This is not inherent to hydrogen combustion, but is instead a consequence of the attempt to produce a systematic study with a laminar flat flame burner. The authors hypothesize that this effect would be eliminated in a more turbulent, practical combustion system.

The hydrogen tests can be summarized as follows. $NO_X$ emissions appear in the public literature as a concern in the case of hydrogen combustion. However, chemical kinetic calculations show that lean premixed hydrogen combustion $NO_X$ emissions are comparable to (and potentially lower than) those of methane combustion at a fixed adiabatic flame temperature and residence time. Experimental measurements demonstrate that low $NO_X$ emissions are in fact achievable with lean premixed hydrogen combustion. Within this low $NO_X$ result, the experiments appear to show higher $NO_X$ than the simulations, and higher $NO_X$ with higher hydrogen. This result appears to be due to the comparison of very small $NO_X$ numbers with extreme sensitivity to experimental uncertainty, with measurement uncertainty and thermodiffusive instability as confounding effects. This result is an update from ongoing and continued refinement of this research.

## 3 Ammonia Combustion Testing

Like with hydrogen combustion, $NO_X$ emissions have been a concern facing ammonia combustion in the public literature. Chemical kinetics calculations have shown promising $NO_X$ emissions below 30 ppm with a staged combustion architecture. The staged architecture has a rich primary zone followed by a long residence time relaxation zone. The relaxation zone provides the time for the rich combustion products to relax to equilibrium where $NO_X$ concentration is low. A lean burnout section introduces additional air to burn out the remaining fuel and achieve the desired global equivalence ratio (i.e. combustor exit temperature). This section presents an experimental effort to assess the $NO_X$ performance of such a combustor architecture with real world mixing and other non-1D effects.

### 3.1 Experimental Setup

The experimental setup consists of a premixed ammonia-air fuel supply with methane blending capability. The combustor utilizes a high swirl swirler with a centerbody. The centerbody is fitted with a spark igniter and hydrogen orifice, which together form a hydrogen torch igniter. This torch is used only for ignition and is off during measurements.

Emissions samples were collected with a water cooled probe. The probe includes a rake tip that samples from multiple locations with a sample port spacing that is designed to provide a spatial average from a circular cross section with a linear array of ports. The probe type includes a water-cooled heat exchanger to reduce the gas temperature to freeze the NO formation chemistry at the point of sampling. A condenser is used to remove water from the sample before analysis. A California Analytical Instruments 700 LX Series NDIR/$O_2$ Analyzer for $O_2$ and 700 FTIR multi-gas analyzer with NO, $NO_2$, $NH_3$, and $N_2O$ measurement capabilities was used to measure emissions concentrations. This paper presents NO and $NO_2$ concentrations together as total $NO_X$. Although outside the scope of this paper, the NO to $NO_2$ balance was also investigated with most of the $NO_X$ composed of NO. Accuracy of this instrument is better than 1% of full scale (0-5000 ppm for $NH_3$ and NO and 0-1000 ppm for $N_2O$ and $NO_2$), repeatability is

better than 0.5% of full scale, and the instrument was calibrated daily on zero gas ($N_2$) and span gases.

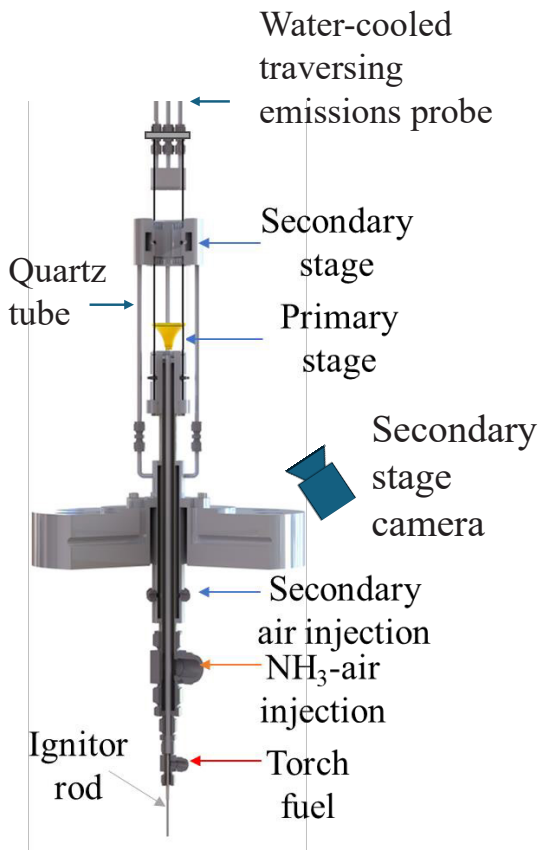


**Figure 6.** Experimental layout of the ammonia combustion test rig

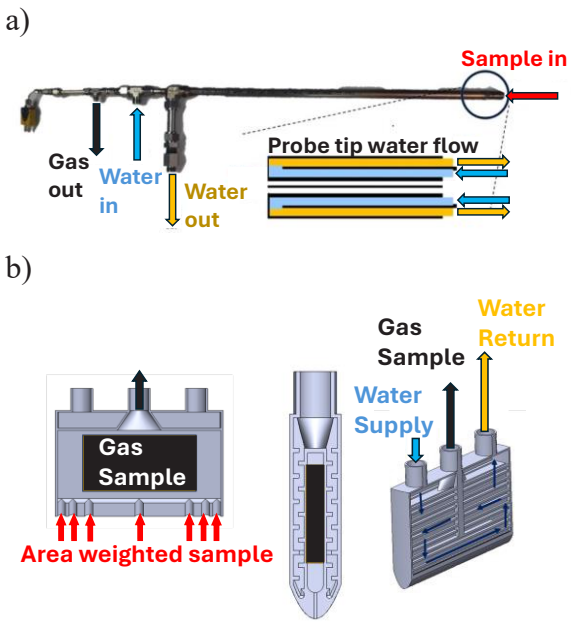


**Figure 7.** Emissions sampling probe a) photograph and b) diagram

### 3.2 Results and Analysis

Experiments were conducted first to characterize the primary (rich) zone flame. A DSLR camera was filtered around 630 nm to collect chemiluminescence images of the $NH_2$* radical. Images were collected at a range of velocities and equivalence ratios. These images are presented in Figure 8. Several flame shapes were identified, including lifted wake-stabilized flames, attached wake-stabilized flames, and attached inner-shear layer flames. For these studies, the rig was operated at conditions that provided an attached inner-shear layer stabilized flame.

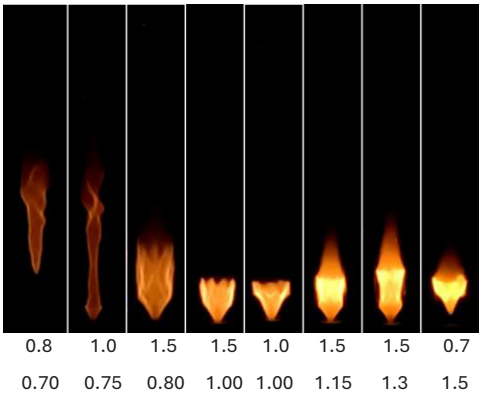


**Figure 8.** Pure ammonia flame shapes from ammonia combustion test rig at various equivalence ratios and nozzle velocities

The secondary (lean) zone consists of an air injection ring. Several air injection configurations were analyzed. These configurations included 5 hole, 10 hole, and 16 hole air injectors. The air injection configurations also included the option for different quench hole diameters to effect the momentum flux ratio of the air jets. The secondary air injection burns as a partially premixed flame, which is mostly fueled by hydrogen from cracked ammonia from the primary stage. Figure 9 shows a sample of DSLR images of the flame shapes in the secondary stage for the three different numbers of air injection holes.

Figure 10 presents the emissions results. The figure is arranged with global equivalence ratio on the horizontal axis, and three different colors representing the three different primary equivalence ratios. On the right side of the figure, data points are plotted that are disjointed from the other measurements. These data points were measured with no secondary air injection; they represent the primary zone emissions contribution. Moving to the left on the plot corresponds to an introduction of and increase in secondary air flow rate, accompanied by a reduction in the global equivalence ratio relative to the primary zone equivalence ratio. The figure shows a step increase in $NO_X$ as secondary air is introduced, due to the thermal $NO_X$ that is produced as the remaining fuel is burned. The figure shows that data tends to cluster together for a given primary equivalence ratio, showing a relative insensitivity to the air injection hardware configuration. Finally, the results show minimized $NO_X$ emissions for the case of a primary

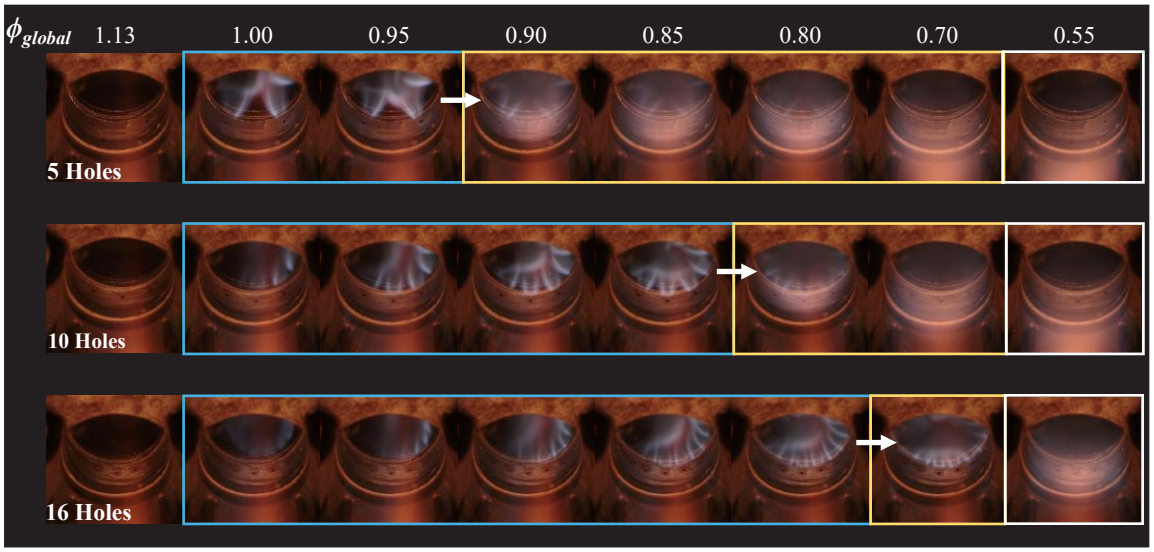


**Figure 9.** Secondary zone flame shapes in ammonia combustion test rig. Primary zone is fueled by 100% ammonia. Results shown for 5, 10, and 16 hole (5H, 10H, and 16H) quench hole configurations with 2.1 mm quench holes, and a range of global equivalence ratios. Yellow vertical lines demarcate transition between mostly non-premixed jet burning and more premixed burning. Figure 6 indicates the position of the secondary zone camera.

equivalence ratio of 1.15, indicating that this is the optimum primary zone equivalence ratio for this study. Global equivalence ratios in the 0.5 to 0.6 vicinity are relevant to frame engine conditions. $NO_X$ emissions on the order of 50 ppm are observed at these conditions.

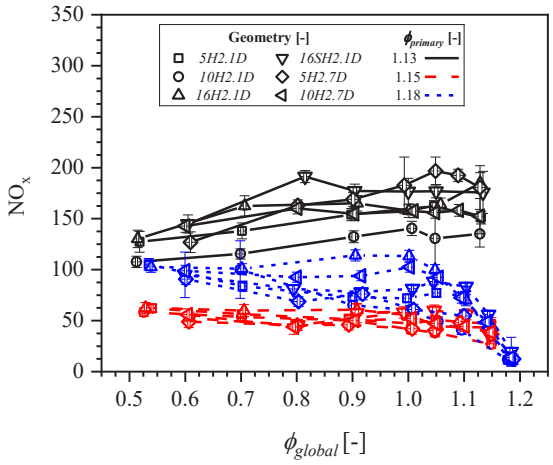


**Figure 10.** $NO_X$ emissions vs global equivalence ratio for various hardware configurations at three different primary zone equivalence ratios. Results shown for various combinations of 5, 10, and 16 hole (5H, 10H, and 16H) quench hole configurations with 2.1 mm and 2.7 mm quench holes (2.1D and 2.7D). The 16SH2.1D configuration has two rows of holes.

In addition to $NO_X$ emissions, ammonia combustion has attracted concern over ammonia slip and $N_2O$ emissions. While characterization of these pollutants is beyond the scope of this paper, these are important considerations that were measured during this study. In general, this combustor produced zero ammonia slip within experimental uncertainty under overall lean operating conditions, and at overall rich conditions it produced $NH_3$ emissions up to roughly 150 ppm at 15% $O_2$. The $N_2O$ emissions were 4 ppm at 15% $O_2$ at overall rich conditions and 2 ppm at 15% $O_2$ at overall lean conditions.

One remaining question surrounding this work is the combustion efficiency of the secondary stage. Combustion efficiency refers to the fraction of unburned fuel in the exhaust gas whose chemical energy is not released in combustion. This remains a question because we hypothesize that most of the unburned ammonia from the primary zone cracks to hydrogen. Consequently, it stands to reason that fuel slip could take the form of hydrogen slip rather than ammonia slip. This is a work in progress, with recent measurements of exhaust gas $O_2$ concentration used as an indicator of secondary zone efficiency. Preliminary results show that higher secondary air flows (corresponding to practical global equivalence ratios) have the best combustion efficiency, probably due to enhanced fluid-dynamic mixing that occurs with higher air flow and higher momentum flux ratio. However, this is still an area of active research which merits direct measurement of the exhaust gas hydrogen concentration.

The results presented here show promise for low $NO_X$ combustion systems with ammonia fuel. It is important to keep in mind that these tests were performed at atmospheric pressure. The chemical kinetics calculations predicted an improvement in emissions at higher pressures due to lower rich zone NO equilibrium concentration and faster relaxation to that rich equilibrium with pressure. This adds additional promise to this combustor architecture for low $NO_X$ ammonia combustion. Operation of this experiment at higher pressures is an ongoing effort and natural next step for this work.

## 4 CONCLUSIONS

Hydrogen and ammonia are both zero carbon fuels that show promise as potential decarbonization pathways for gas turbines. However, both of these fuels have been scrutinized over potential $NO_X$ emissions concerns. Much of this scrutiny stems from a misunderstanding of $NO_X$ formation mechanisms, and experimentation with new fuels in legacy hardware. The 2023 IGTC conference [26] and recent publications have shown chemical kinetic calculations that demonstrate the potential for reasonable $NO_X$ emissions from both of these fuels. In the case of hydrogen, a premixed flame with a fixed adiabatic flame temperature and residence time should have $NO_X$ emissions that are insensitive to fuel type (for non-nitrogen containing fuels). In the case of ammonia, an RRQL combustor architecture has potential for low double digit $NO_X$. This paper presents experimental updates in response to those calculations. In the case of hydrogen, the experiments presented challenges with instrumentation uncertainty and thermodiffusive instabilities which challenged the fine control of flame temperature. Nevertheless, the experiments demonstrated low $NO_X$ with lean premixed hydrogen. In the case of ammonia, double-digit $NO_X$ is demonstrated with an RRQL combustor at atmospheric pressure, with lower $NO_X$ expected at higher pressures. This paper provides an update from the continued developments of both of these experiments. These experimental observations are important as their results show that the community should not villainize these fuels on the basis of $NO_X$ emissions. Instead, the community should focus engineering efforts on re-architecting gas turbine combustors specifically for these fuels.

## REFERENCES

[1] T. Lieuewen, M. Chang and A. Amato, "Stationary gas turbine combustion: Technology needs and policy considerations," *Combustion and Flame,* vol. 8, no. 160, p. 1311–1314, 2013.

[2] L. Davis and R. Washam, "Development of a dry low nox combustor," in *Turbo Expo: Power for Land, Sea, and Air, American Society of Mechanical Engineers*, 1989. Paper no 89-GT-255.

[3] P. Stuttaford, H. Rizkalla, Y. Chen, B. Copley and T. Faucett, "Extended turndown, fuel flexible gas turbine combustion system," in *Turbo Expo: Power for Land, Sea, and Air*, 2010. Paper no GT2010-22585.

[4] B. Lacy, W. Ziminsky, J. Lipinski, B. Varatharajan, E. Yilmaz and a. J. Brumberg, "Low emissions combustion system development for the GE energy high hydrogen turbine program," in *Turbo Expo: Power for Land, Sea, and Air*, 2008. Paper no GT2008-50823.

[5] A. Campbell, J. Goldmeer, T. Healy, R. Washam, M. Moliere and J. Citeno, "Heavy duty gas turbines fuel flexibility," in *Turbo Expo: Power for Land, Sea, and Air*, 2008. Paper no GT2008-51368.

[6] G. J. Rørtveit, K. Zepter, Ø. Skreiberg, M. Fossum and J. E. Hustad, "A comparison of low-nox burners for combustion of methane and hydrogen mixtures," *Proceedings of the Combustion Institute,* vol. 29, no. 1, p. 1123–1129, 2002.

[7] W. D. York, W. S. Ziminsky and E. Yilmaz, "Development and testing of a low nox hydrogen combustion system for heavy duty gas turbines," in *Turbo Expo: Power for Land, Sea, and Air*, 2012. Paper no GT2012-69913.

[8] M. Waslo and J. Hilt, "Evolution of nox abatement techniques through combustor design for heavy-duty gas turbines," *J. Eng. Gas Turbines Power,* vol. 106, no. 4, 1984.

[9] G. Leonard and J. Stegmaier, "Development of an aeroderivative gas turbine dry low emissions combustion system," *J. Eng. Gas Turbines Power,* vol. 116, no. 3, 1994.

[10] A. C. Lewis, "Optimising air quality co-benefits in a hydrogen economy: A case for hydrogen-specific standards for NOx emissions," *Environmental Science: Atmospheres,* vol. 1, no. 5, p. 201–207, 2021.

[11] O. Tuncer, "The effect of hydrogen enrichment of methane fuel on flame stability and emissions," in *International Conference on Renewable Energy Research and Applications (ICRERA)*, 2013.

[12] P. Therkelsen, T. Werts, V. McDonell and S. Samuelsen, "Analysis of nox formation in a hydrogen-fueled gas turbine engine," 2009.

[13] M. S. Cellek and A. Pınarba, "Investigations on performance and emission characteristics of an industrial low swirl burner while burning natural gas, methane, hydrogen-enriched natural gas and hydrogen as fuels," *International Journal of Hydrogen Energy,* vol. 43, no. 2, 2018.

[14] T. Bullard, A. Steinbrenner, P. Stuttaford, D. Jansen and T. d. Bruijne, "Improvement of premixed gas turbine combustion system fuel flexibility with increased hydrogen consumption in a renewable market place," in *Turbo Expo: Power for Land, Sea, and Air*, 2018. Paper no GT2018-75553.

[15] M. Ilbas and I. Yılmaz, "Experimental analysis of the effects of hydrogen addition on methane combustion," *International Journal of Energy Research,* vol. 36, no. 5, p. 643–647, 2012.

[16] S. Cocchi, M. Provenzale, V. Cinti, L. Carrai, S. Sigali and D. Cappetti, "Experimental characterization of a hydrogen fuelled combustor with reduced nox emissions for a 10 MW class gas turbine," in *Turbo Expo: Power for Land, Sea, and Air*, 2008. Paper no GT2008-51271.

[17] F. Hernandez and H. Rizkalla, "Retrofittable solutions to keep existing gas turbine power plants viable and profitable in an increasingly dynamic power generation market: Validation of low pressure drop flamesheet™ combustor," in *Turbo Expo: Power for Land, Sea, and Air*, 2019. Paper no GT2019-91647.

[18] P. Chiesa, G. Lozza and L. Mazzocchi, "Using hydrogen as gas turbine fuel," *Journal of Engineering for Gas Turbines and Power,* vol. 127, no. 1, p. 73–80, 2005.

[19] P. Glanville, "Impact of hydrogen/natural gas blends on partially premixed combustion equipment: Nox emission and operational performance," *Energies,* vol. 15, no. 5, p. 1706, 2022.

[20] B. Breer, H. Rajagopalan, C. Godbold, H. Johnson, B. Emerson, V. Acharya, W. Sun, D. Noble and T. Lieuwen, "Numerical Investigation of NOx Production from Premixed Hydrogen/Methane Fuel Blends," *Combustion and Flame,* vol. 255, p. 112920, 2023.

[21] C. M. Douglas, S. L. Shaw, T. D. Martz, R. C. Steele, D. R. Noble, B. L. Emerson and T. C. Lieuwen, "Pollutant Emissions Reporting and Performance Considerations for Hydrogen–Hydrocarbon Fuels in Gas Turbines," *Journal of Engineering for Gas Turbines and Power,* vol. 144, no. 9, 2022.

[22] S. Ito, M. Uchida, S. Kato, T. Fujimori and H. Kobayashi, "Emission characteristics of a lean-premixed ammonia/natural-gas gas-turbine combustor and effect of secondary ammonia injection," *Mechanical Engineering Journal,* vol. 6, no. 5, 2019.

[23] M. A. Nose, T. O. Kawakami, S. O. Nakamura, H. Kuroki, M. Kataoka and M. Yuri, "Development of hydrogen/ammonia firing gas turbine for decarbonized society," *Mitsubishi Heavy Ind. Tech. Rev,* 2021.

[24] C. D. A. Jimenez, "PhD Dissertation: Experimental Assessment of a Micro Gas Turbine Running on Ammonia-based Fuel Blends," KAUST, 2023.

[25] A. M. Elbaz, Z. O. Hassan, A. M. Albalawi and W. L. Roberts, "Report: Emissions, Stability, and Flame Structure of KAUST Double Swirl Burner (KDSB) Fired With Ammonia/Methane Blends," in *American Flame Research Committee, AFRC Symposium Papers*, 2023.

[26] S. Gubbi, R. Cole, B. Emerson, D. Noble, R. Steele, W. Sun and T. Lieuwen, "Evaluation of Minimum NOx Emission from Ammonia Combustion," in *11th IGTC*, Brussels, Belgium, 2023.